Host–Guest Systems

Deutsche Ausgabe: DOI: 10.1002/ange.201502047
Internationale Ausgabe: DOI: 10.1002/anie.201502047

# A Universal Strategy for Aptamer-Based Nanopore Sensing through Host–Guest Interactions inside α-Hemolysin**

*Ting Li, Lei Liu, Yuru Li, Jiani Xie, and Hai-Chen Wu**

***Abstract:*** *Nanopore emerged as a powerful single-molecule technique over the past two decades, and has shown applications in the stochastic sensing and biophysical studies of individual molecules. Here, we report a versatile strategy for nanopore sensing by employing the combination of aptamers and host–guest interactions. An aptamer is first hybridized with a DNA probe which is modified with a ferrocene⊂cucurbit-[7]uril complex. The presence of analytes causes the aptamer–probe duplex to unwind and release the DNA probe which can quantitatively produce signature current events when translocated through an α-hemolysin nanopore. The integrated use of magnetic beads can further lower the detection limit by approximately two to three orders of magnitude. Because aptamers have shown robust binding affinities with a wide variety of target molecules, our proposed strategy should be universally applicable for sensing different types of analytes with nanopore sensors.*

The ability of sensing individual molecules is highly desirable in modern biology, chemistry, and their interfaces.[1] Among currently available single-molecule techniques, stochastic sensing with nanopores has attracted much attention since its emergence in the late-1990s.[2,3] The principle of nanopore sensing is to monitor the ionic current fluctuation through nanopores when an analyte binds with the pore. The current amplitude change and the mean dwell time of the analyte binding reveal its identity, whereas the frequency of the binding events reveals the analyte concentration.[4] The diameters of naturally occurring protein nanopores are generally within the range of a few nanometers, which endows them with very high sensitivity in sensing ions[5] and small molecules.[3,6] However, for bulky analytes such as proteins which are too large to bind within the lumen of the protein pores, there have been various approaches in literature to transmit binding events arising outside the pore to the interior so that the ionic current is modulated.[7] In this regard, solid-state nanopores possess intrinsic advantages with tunable pore size and shape. However, it remains challenging to control the surface chemistry of the pore wall and maintain single-molecule sensitivity in surface-modified solid-state nanopores.[8] New types of nanopores developed in the past decade have been mainly focused on the analyses of nucleic acids, and full exploration of their potentials in stochastic sensing is still underway.[9] Therefore, an effective nanopore sensing method that can sensitively detect proteins, nucleic acids and small molecule analytes has still remained elusive.

In this report, we develop a universal strategy for nanopore sensing by employing the combination of aptamers and host–guest interactions.[10] The principle that underlies the strategy is shown in Figure 1. Aptamers are single-stranded oligonucleic acids that bind to specific target molecules with high affinities.[11] In the proposed strategy, we first hybridize an aptamer with a DNA probe which is fully complementary to the aptamer or contains a few deliberate mismatches. The DNA probe, modified with a host–guest complex in the middle of the strand, is envisioned to generate characteristic current events when it passes through αHL (Figure 2a). Since DNA duplex is too large to traverse through αHL pore, no translocation events could be observed when the aptamer–probe duplex is subjected to a translocation test. However, the presence of analyte may cause the aptamer–probe duplex to unwind if the binding affinity of the analyte–aptamer is higher than that of the duplex. This process eventually frees the DNA probe which would generate characteristic current events when translocated through αHL under the transmembrane potential (Figure 1). By employing this strategy, we have successfully detected vascular endothelial growth factor (VEGF), thrombin, and cocaine with high levels of sensitivity. In addition, the integrated use of magnetic beads can further lower the detection limit by approximately two to three orders of magnitude. Because aptamers have shown robust binding affinities with a wide variety of target

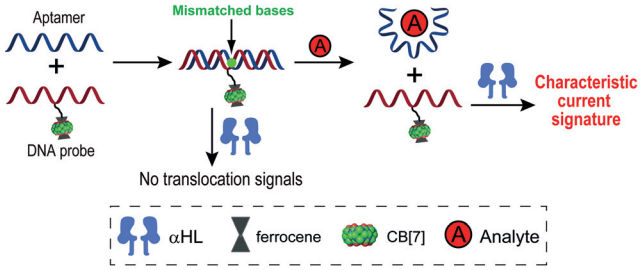


***Figure 1.*** The proposed sensing strategy. The icon legends are shown in the dashed rectangle box.

[*] T. Li,[+] Dr. L. Liu,[+] Y. Li, J. Xie, Prof. Dr. H.-C. Wu
Key Laboratory for Biomedical Effects of Nanomaterials & Nanosafety, Institute of High Energy Physics
Chinese Academy of Sciences
Beijing 100049 (China)
E-mail: haichenwu@ihep.ac.cn

[+] These authors contributed equally to this work.

[**] We thank Prof. E. K. Wang (CIAC) for the cocaine sample and Prof. Q. S. Liu (IHEP) for providing αHL mutants used in this work. This project was funded by National Basic Research Program of China (973 program, numbers 2013CB932800), the National Natural Science Foundation of China (numbers 21175135, 21375130, 21205119, 21475132), and the CAS Hundred Talents Program.

Supporting information for this article is available on the WWW under http://dx.doi.org/10.1002/anie.201502047.

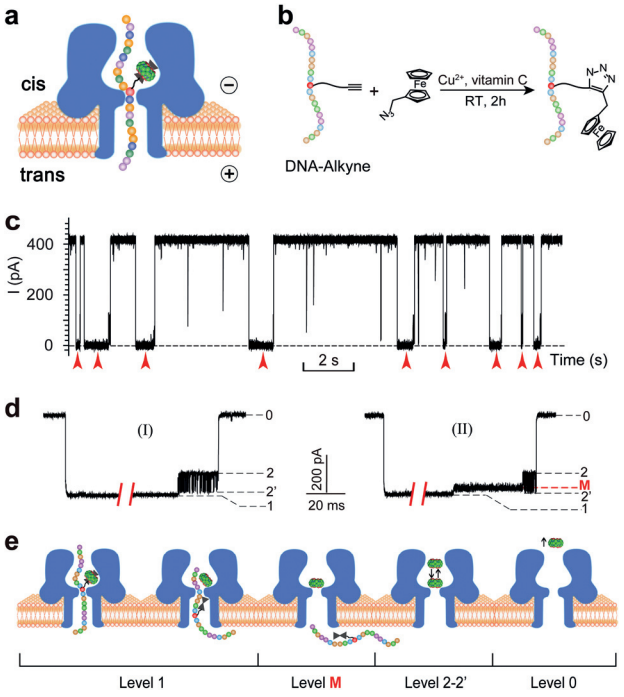


***Figure 2.*** Translocation of Fc⊂CB[7]-modified ssDNA through αHL. a) The translocation of an Fc⊂CB[7]-modified DNA molecule through αHL nanopore. b) Chemical modification of the alkyne-containing ssDNA through click chemistry to attach an Fc moiety. c) A representative current trace of the translocation of DNA1-Fc⊂CB[7] (final concentration 0.25 μM) through αHL. The red arrows indicate multilevel current events. Data were acquired in the buffer of 3 M KCl and 10 mM Tris, pH 8.0, with the transmembrane potential held at +160 mV. d) Two types of signature events generated during the translocation of DNA1-Fc⊂CB[7]. e) Diagram showing the molecular mechanism of hybrid trapping, dissociation, and translocation, as well as CB[7] oscillation in the vestibule. The sequence of DNA1: 5′-CATATTA-CACT*CCCACGACTC-3′, T* stands for the alkyne-containing thymine.

molecules, our proposed strategy should be generally useful in sensing different types of analytes with nanopore sensors.

We chose one type of commercially available alkyne-containing thymine (T*, for the structure see Table S1) as the key modified base to construct DNA probes. The T* base was normally placed in the middle of the probe strand, and the rest of the sequence of the probe was designed according to the aptamer used for binding the target. The terminal alkyne group on the side chain of T* enables "click" chemistry to attach a "guest" moiety which can catch a "host" molecule in solution to form the host–guest modification (Figures 2b, S1, and S2). We first used the hybrid of DNA1-adamantane⊂β-cyclodextrin (Ad⊂βCD) to examine the translocation signals (for DNA sequences, see Table S1). Translocation of the DNA hybrid through αHL was conducted in 3 M KCl, 10 mM Tris at pH 8.0 with the transmembrane potential held at +160 mV. After the hybrid (final concentration 0.25 μM) was placed in the *cis* compartment, we observed moderately long current blockades ($\tau_{off} = 37.7 \pm 2.4$ ms) with virtually no residual current remaining (Figure S3). Although those events are clearly different from single-stranded DNA (ssDNA) translocation events, the detection might be interfered with by analytes that bind with αHL and cause large current blockades. Next, we tested another hybrid DNA1-ferrocene⊂cucurbit[7]uril (Fc⊂CB[7]) for translocation through αHL under the same conditions. Interestingly, we observed highly characteristic current events at the frequency of 16.8 $min^{-1}$ (Figure 2c). Among them, there are two types of slightly different signature events that were named type-I and type-II (2.65:1), respectively (Figure 2d). Type-I events are composed of two consecutive parts with level 1 featuring long and deep blockades and level 2-2′ featuring transient current oscillations, whereas type-II events have the similar pattern except for an additional intermediate current level (level M, Figure 2d). The molecular mechanism of DNA hybrid translocation is summarized in Figure 2e. Figure 3a illustrates a typical type-II event with all parameters labeled. The scatter plots of residual current versus duration of the levels 1, M, and 2 in both type-I and type-II events are shown in Figure 3b. It was found that the scatter plots of the levels 1 and 2 in the two types of signature events nicely overlapped with each other. The histograms of the current blockage of each level were shown in Figure 3c and the dwell time histograms of each level in Figure 3d–f.

We have performed detailed experiments to confirm the assignments of each current level in signature events (Supporting Information S5–S8). We attributed the level 1 state to the translocation of DNA1-Fc⊂CB[7] and concomitant dissociation of the Fc⊂CB[7] complex at the constriction of αHL (Figures S4 and S5). By protein mutant experiments, we

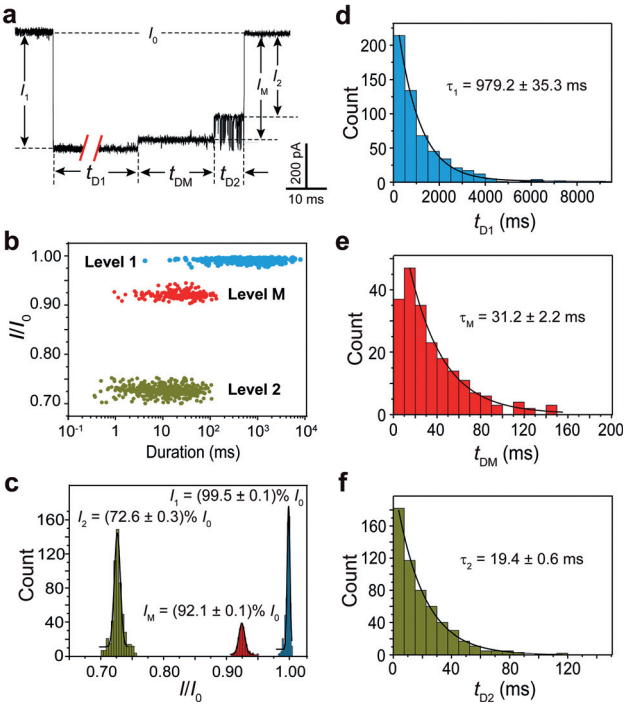


***Figure 3.*** Statistical analysis of the signature events. a) A typical type-II signature event during the translocation of DNA1-Fc⊂CB[7] through αHL under the identical conditions in Figure 2. $I_0$ stands for open pore current; $I_{1\text{-}2}$ stands for the most probable current blockade of level 1-2; $t_{D1\text{-}2}$ stands for the duration of the level 1-2. b) Scatter plots showing current blockades versus event durations of levels 1–2 in the signature events. The number of events is 500. c) Histograms of the current blockades of level 1-2. The solid lines are Gaussian fit to the histograms. d–f) Dwell time histograms of level 1-2. The solid lines are the single exponential fit to the histograms.

confirmed that the level 2-2′ alternation was due to the trapping and oscillation of CB[7] inside the vestibule of αHL (Figures S6 and S7), whereas level M was caused by the stochastic binding of CB[7] with amino acid residues in the constriction region of αHL (Figure S8). The association of the signature events with CB[7] was further confirmed by a competing experiment by adding 1-aminoadamantane to the solution of DNA1-Fc⊂CB[7] during translocation studies (Figure S9). This result provided additional evidence that the unique pattern of the signature events is caused by the trapping of CB[7] in the vestibule of αHL.

To examine the versatility of the sensing strategy, we tested several different types of analytes. The first model molecule we chose is $VEGF_{121}$. VEGF regulates early embryogenesis through vasculogenesis and angiogenesis, and is an important biomarker for different clinical disorders.[12] Currently available analytical methods for quantitative detection of VEGF include ELISA assays,[13] fluorescence binding assay,[14] electrochemical analysis,[15] and optical aptasensors.[16] In the present work, we first hybridized VEGF aptamer DNA2 with equimolar Fc⊂CB[7]-modified probe DNA3 in solution. There are three mismatched base pairs between DNA2 and DNA3 which facilitates the competitive binding of $VEGF_{121}$ (Tables S1 and S2). When this DNA duplex was subjected to αHL for the translocation test, we observed no ssDNA translocation signals. After $VEGF_{121}$ was added to the solution and incubated for 2 h, characteristic multilevel events started to appear. The occurrence of the signature events could be correlated with the presence of $VEGF_{121}$, and thus their frequency ($f_{sig}$) can be used to quantify the concentration of $VEGF_{121}$. We constructed the standard working curves of $f_{sig}$ versus different concentrations of $VEGF_{121}$ (Figure 4a). It is found that $f_{sig}$ increases as the concentration of $VEGF_{121}$ is elevated, and reaches a plateau at around 200 nM. In the low concentration region, $VEGF_{121}$ can be unambiguously detected as low as 0.5 nM by the standard procedure. To corroborate the above results, we carried out the control experiment and examined the selectivity of the assay toward $VEGF_{121}$. We added bovine serum albumin (BSA), lysozyme, or thrombin instead of $VEGF_{121}$ into the aptamer-probe solution, respectively. The results showed that the $f_{sig}$ in the interferential protein groups is almost as high as the control group. Thus, those proteins do not interfere with the detection of $VEGF_{121}$ (Figure 4b).

We have also successfully achieved the detection of thrombin (5–100 nM) and cocaine (5–500 μM) with the developed strategy and the results are shown in Figures S11 and S12. The detection limits of the aptamer-based nanopore sensing strategy for protein analytes and small molecules are comparable with those of literature methods, especially fluorescence spectroscopy.[11,16] However, the detection sensitivity at the nanomolar range is not sufficiently high for sensing clinically relevant protein biomarkers.[17] Thus, we set out to improve the sensitivity of the strategy and further lower the detection limits. During the detection of different analytes by the aptamer-based approach, we found that the presence of excess aptamer–probe duplexes in solution could severely disturb the recording of characteristic events produced by the Fc⊂CB[7]-modified DNA probes. On one hand, although the

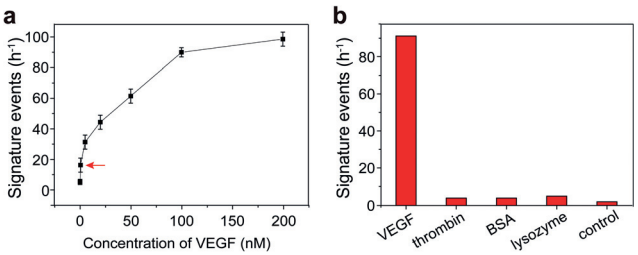


***Figure 4.*** Quantitative determination of $VEGF_{121}$. a) Correlation of the frequency of signature events ($f_{sig}$) with the concentration of $VEGF_{121}$ (0.5, 5, 20, 50, 100, 200 nM). Number of individual experiments $n = 6$. b) Investigation of the selectivity in the detection of $VEGF_{121}$. The final concentration of $VEGF_{121}$ is 10 nM, whereas the concentration of thrombin, BSA, and lysozyme is 10 μM each. All data were acquired in the buffer of 3 M KCl and 10 mM tris, pH 7.2, with the transmembrane potential held at +160 mV.

aptamer–probe duplexes do not unwind and traverse through αHL, they could lodge in the vestibule and produce long-lasting events (Figure S12a).[18] Those events were generally several seconds long and sometimes caused current blockage that required potential reversal. On the other hand, the aptamer–probe duplexes competed with the DNA probes for occupation in αHL, which drastically reduced the efficiency of the generation of signature events. This situation deteriorates when the analyte concentration is relatively low while the aptamer–probe duplexes are in large excess. Therefore, eliminating the interference of the aptamer–probe duplexes might greatly improve detection limits of the approach.

Magnetic particles of micron scale have been widely used in ultrasensitive bioanalyte detection owing to their capacity of facilitating the collection of captured molecules. Here we used one kind of superparamagnetic beads of 1.0 μm in diameter with a streptavidin monolayer covalently coupled to the hydrophilic bead surface in the detection of $VEGF_{121}$. First, we attached a biotin moiety to the 3′ of the new aptamer DNA8. After the biotinylated aptamer was hybridized with the probe DNA3-Fc⊂CB[7], magnetic beads (MBs) were added to this solution and incubated for 20 min. MBs were collected using a magnetic field and washed with deionized water (step 1). Next, we incubated $VEGF_{121}$ with MBs, leading to the release of DNA3-Fc⊂CB[7] (step 2). Then, a magnetic field was applied to remove all the MBs from the solution (step 3). Finally, only the DNA3-Fc⊂CB[7] was left in the solution for the single-channel recording experiments (step 4; Figure 5a). Following this procedure, we conducted the detection of different concentrations of $VEGF_{121}$ within the range of 0–500 pM. We found that all the recording traces became much cleaner after MBs treatment (Figure S12c). Interestingly, the $f_{sig}$ exhibited a linear relationship with the concentration of $VEGF_{121}$ in the range of 5 pM and 500 pM (Figure 5b). Since the control experiment gave a quite clean background owing to the usage of MBs, the detection limit of the MB-assisted sensing approach for $VEGF_{121}$ is at the picomolar level. This value is certainly adequate for analyzing VEGF-related clinical samples. We also performed selectivity studies in the MB-assisted assay and found that $f_{sig}$ of the interfering groups was no higher than that of the control group (Figure 5c).

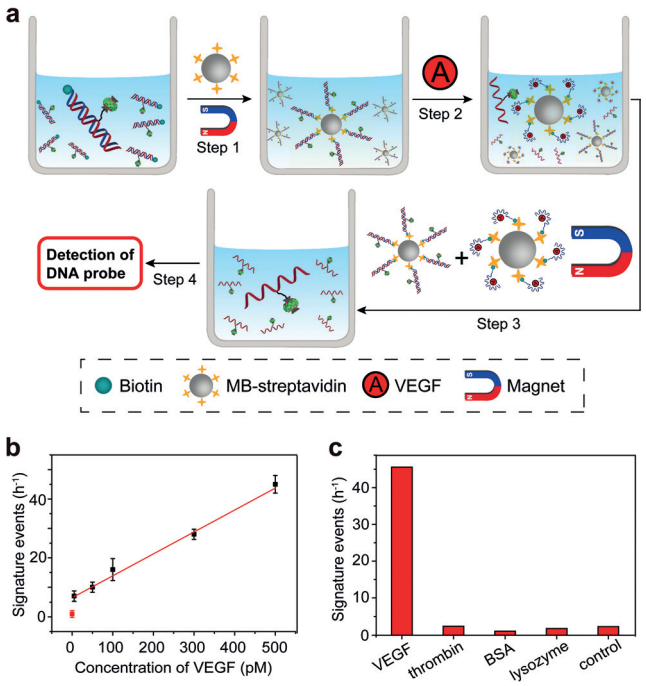


***Figure 5.*** Improved detection of $VEGF_{121}$ by using MBs. a) Illustration of the application of MBs in improving the sensitivity of $VEGF_{121}$ detection. The icon legends are shown in the dashed rectangle box. b) Correlation of the frequency of signature events ($f_{sig}$) with the concentration of $VEGF_{121}$ within the range of 0–500 pM (final concentration: 5, 50, 100, 300, 500 pM). The data could be fitted with a linear equation $f_{sig} = 0.0746*[VEGF] + 6.42$, $R = 0.998$. The red spot is the data of the control group. c) Selectivity studies in the detection of $VEGF_{121}$ with MBs. All data were acquired in the buffer of 3 M KCl and 10 mM tris, pH 7.2, with the transmembrane potential held at +160 mV. Number of individual experiments $n = 3$.

In summary, we have developed a versatile aptamer-based nanopore sensing approach for the detection of proteins and small organic molecules. The host–guest (Fc⊂CB[7]) complex attached on the DNA is crucial for the generation of characteristic events. Experimental data have shown that the serendipitous use of CB[7] is imperative for producing the unique current pattern in signature events. This feature endows the detection with very high confidence at the single-molecule level. By modulating the interplay between aptamer length, binding affinities, and mismatches in the aptamer–probe duplexes, we can virtually turn this aptamer-based sensing approach into a universal methodology for detecting different classes of analytes. The integrated use of magnetic beads can eliminate the interference of excess aptamer–probe duplexes and further lower the detection limit by approximately two to three orders of magnitude. With further investigation of the generation of different signature events, it will be possible to build nanopore sensors for the detection of a variety of analytes in a single sample.

**Keywords:** aptamers · host–guest systems · magnetic beads · nanopore sensors · quantitative determination

**How to cite:** *Angew. Chem. Int. Ed.* **2015**, *54*, 7568–7571
*Angew. Chem.* **2015**, *127*, 7678–7681

[1] a) J. Zlatanova, K. van Holde, *Mol. Cell* **2006**, *24*, 317–329; b) H. Bayley, T. Luchian, S.-H. Shin, M. B. Steffensen, *Single Molecules and Nanotechnology, Vol. 24* (Eds.: R. Rigler, H. Vogel), Springer, Heidelberg, **2008**, pp. 251–277.
[2] J. J. Kasianowicz, E. Brandin, D. Branton, D. W. Deamer, *Proc. Natl. Acad. Sci. USA* **1996**, *93*, 13770–13773.
[3] L. Q. Gu, O. Braha, S. Conlan, S. Cheley, H. Bayley, *Nature* **1999**, *398*, 686–690.
[4] H. Bayley, P. S. Cremer, *Nature* **2001**, *413*, 226–230.
[5] a) O. Braha, L. Q. Gu, L. Zhou, X. F. Lu, S. Cheley, H. Bayley, *Nat. Biotechnol.* **2000**, *18*, 1005–1007; b) A. F. Hammerstein, S.-H. Shin, H. Bayley, *Angew. Chem. Int. Ed.* **2010**, *49*, 5085–5090; *Angew. Chem.* **2010**, *122*, 5211–5216.
[6] H.-C. Wu, H. Bayley, *J. Am. Chem. Soc.* **2008**, *130*, 6813–6819.
[7] a) L. Movileanu, S. Howorka, O. Braha, H. Bayley, *Nat. Biotechnol.* **2000**, *18*, 1091–1095; b) S. Howorka, J. Nam, H. Bayley, D. Kahne, *Angew. Chem. Int. Ed.* **2004**, *43*, 842–846; *Angew. Chem.* **2004**, *116*, 860–864.
[8] R. Wei, V. Gatterdam, R. Wieneke, R. Tampe, U. Rant, *Nat. Nanotechnol.* **2012**, *7*, 257–263.
[9] a) T. Z. Butler, M. Pavlenok, I. M. Derrington, M. Niederweis, J. H. Gundlach, *Proc. Natl. Acad. Sci. USA* **2008**, *105*, 20647–20652; b) D. Wendell, P. Jing, J. Geng, V. Subramaniam, T. J. Lee, C. Montemagno, P. Guo, *Nat. Nanotechnol.* **2009**, *4*, 765–772; c) S. Garaj, W. Hubbard, A. Reina, J. Kong, D. Branton, J. A. Golovchenko, *Nature* **2010**, *467*, 190–193; d) G. F. Schneider, S. W. Kowalczyk, V. E. Calado, G. Pandraud, H. W. Zandbergen, L. M. K. Vandersypen, C. Dekker, *Nano Lett.* **2010**, *10*, 3163–3167; e) C. A. Merchant, K. Healy, M. Wanunu, V. Ray, N. Peterman, J. Bartel, M. D. Fischbein, K. Venta, Z. Luo, A. T. C. Johnson, M. Drndic, *Nano Lett.* **2010**, *10*, 2915–2921; f) L. Liu, C. Yang, K. Zhao, J. Li, H.-C. Wu, *Nat. Commun.* **2013**, *4*, 2989; g) M. Langecker, V. Arnaut, T. G. Martin, J. List, S. Renner, M. Mayer, H. Dietz, F. C. Simmel, *Science* **2012**, *338*, 932–936; h) S. Liu, B. Lu, Q. Zhao, J. Li, T. Gao, Y. Chen, Y. Zhang, Z. Liu, Z. Fan, F. Yang, L. You, D. Yu, *Adv. Mater.* **2013**, *25*, 4549–4554; i) J. Geng, K. Kim, J. Zhang, A. Escalada, R. Tunuguntla, L. R. Comolli, F. I. Allen, A. V. Shnyrova, K. R. Cho, D. Munoz, Y. M. Wang, C. P. Grigoropoulos, C. M. Ajo-Franklin, V. A. Frolov, A. Noy, *Nature* **2014**, *514*, 612–615; j) K. Liu, J. Feng, A. Kis, A. Radenovic, *ACS Nano* **2014**, *8*, 2504–2511.
[10] a) O. Braha, J. Webb, L. Q. Gu, K. Kim, H. Bayley, *ChemPhysChem* **2005**, *6*, 889–892; b) Y.-L. Ying, J. Zhang, F.-N. Meng, C. Cao, X. Yao, I. Willner, H. Tian, Y.-T. Long, *Sci. Rep.* **2013**, *3*, 1662.
[11] E. J. Cho, J.-W. Lee, A. D. Ellington, *Annu. Rev. Anal. Chem.* **2009**, *2*, 241–264.
[12] A. Hoeben, B. Landuyt, M. S. Highley, H. Wildiers, A. T. Van Oosterom, E. A. De Bruijn, *Pharmacol. Rev.* **2004**, *56*, 549–580.
[13] P. Scapini, F. Calzetti, M. A. Cassatella, *J. Immunol. Methods* **1999**, *232*, 121–129.
[14] Y. Suzuki, K. Yokoyama, *ChemBioChem* **2009**, *10*, 1793–1795.
[15] S. Prabhulkar, S. Alwarappan, G. Liu, C.-Z. Li, *Biosens. Bioelectron.* **2009**, *24*, 3524–3530.
[16] R. Freeman, J. Girsh, A. F.-j. Jou, J.-a. A. Ho, T. Hug, J. Dernedde, I. Willner, *Anal. Chem.* **2012**, *84*, 6192–6198.
[17] S. O. Kelley, C. A. Mirkin, D. R. Walt, R. F. Ismagilov, M. Toner, E. H. Sargent, *Nat. Nanotechnol.* **2014**, *9*, 969–980.
[18] W. Vercoutere, S. Winters-Hilt, H. Olsen, D. Deamer, D. Haussler, M. Akeson, *Nat. Biotechnol.* **2001**, *19*, 248–252.

Received: March 4, 2015
Revised: April 2, 2015
Published online: May 12, 2015